学　位　論　文

Cl^- channels regulate lipid droplet formation via Rab8a expression during adipocyte differentiation

（Cl^- channels は脂肪細胞分化過程において Rab8a の発現を介して油滴形成を制御する）

福島県立医科大学大学院医学研究科
分子機能学分野 細胞統合生理学講座
大内　佳奈江

論　文　内　容　要　旨（和文）

学位論文題名	Cl^- channels regulate lipid droplet formation via Rab8a expression during adipocyte differentiation Cl^- チャネルは脂肪細胞分化過程において Rab8a の発現を介して油滴形成を制御する

背景：

Cl^-チャネルは、細胞の分化、容積調節、移動、増殖、小胞の酸性化に重要な役割を果たしている。特に、細胞分化においては、Cl^-チャネルが幾つかの細胞内シグナルを活性化させることで、分化を引き起こすことが報告されている。ClC-3 は RUNX2 (runt-related transcription factor 2)経路を介した骨細胞分化に関与し、CFTR (cystic fibrosis transmembrane conductance regulator)は Wnt/βcatenin 経路を介して胚性幹細胞から中内胚葉への分化に関与していることが報告されている。しかしながら、Cl^-チャネルと脂肪細胞分化の関係性は明らかになっていない。本研究の目的は、自己複製能と多分化能を併せ持つ脂肪組織由来幹細胞 (adipose tissue-derived stem cells ; ASCs) と Cl^- チャネルブロッカーを用いて、脂肪細胞分化における Cl^-チャネルの役割を明らかにすることである。

方法：

ウサギの脂肪組織からコラゲナーゼタイプ I を用いて ASCs を単離し、RT-PCR、免疫染色、フローサイトメーターによって ASCs の性状解析を行った。単離した ASCs を脂肪細胞分化誘導培地と Cl^-チャネルブロッカーである NPPB を用いて 7 日間培養した。ASCs、NPPB 未処理の分化細胞 (control)、NPPB で処理した分化細胞から RNA を回収し、リアルタイム RT-PCR によって ASCs マーカー (CD44, SMA, Vimentin)、脂肪細胞マーカー (FAS, adiponectin) の発現量を比較した。さらに、脂肪滴 (lipid droplets ; LDs) と LDs 融合に関わる Rab8a の発現量をリアルタイム RT-PCR と免疫染色によって解析した。また、Cl^-チャネルブロッカーは、液胞型 H^+ ATPase (V-ATP ase)による H^+輸送と共役した ClC Cl^-チャネルによるアニオン輸送を阻害することで小胞内の酸性化に影響することが報告されている。このため、V-ATPase 阻害剤である Bafilomycin を用いて分化誘導を行い、LDs 形成と小胞内酸性化の関係性を pH 感受性蛍光色素である BCECF-AM を用いて評価した。

結果：

単離した ASCs は、ASCs マーカーの発現がみられ、ほとんどの細胞において CD44 陽性細胞であった。7 日間の分化誘導後、未処理の control と NPPB を処理した分化細胞は、ASCs に比べて ASCs マーカーの発現量低下及び脂肪細胞マーカーの発現量上昇が確認されたことから脂肪細胞への分化が示唆された。一方で、未処理の control と NPPB を処理した分化細胞間においては有意な差は確認されず、細胞の形態も同等であったことから NPPB による脂肪細胞分化への影響はなかったことが示唆された。しかしながら、NPPB を処理した分化細胞において、LDs サイズ及び LDs 融合に関与する Rab8a の発現量が control に比べ低下した。さらに、NPPB 以外の Cl^-チャネルブロッカーである DIDS、IAA-94 及び Bafilomycin で処理した分化細胞においても、LDs サイズの減少及び Rab8a の発現量が低下し、細胞内 pH は control に比べて酸性側へ移行した。

結論：

Cl^- チャネルは脂肪細胞分化には関与せず、Rab8a 発現と細胞内小胞の酸性化を介した LDs 形成に関与していることが示唆された。

(Bioscience, Biotechnology, and Biochemistry, 2020, 84, 247-255, Published Online 10 Oct, 2019)

ABSTRACT

Several studies have shown that Cl^- channels regulate the differentiation of some cell types. Thus, I investigated the role of Cl^- channels on adipocyte differentiation using adipose tissue-derived stem cells (ASCs) and Cl^- channel blocker. I induced rabbit ASCs into adipocytes using Cl^- channel blocker. The expression levels of adipocyte markers were no significant difference between the cells treated with a Cl^- channel blocker NPPB and untreated cells. However, when the cells were treated with NPPB, lipid droplets (LDs) sizes decreased compared with the untreated control. Interestingly, the expression levels of Rab8a, which is known as a regulator of LD fusion, were also decreased in the cells treated with NPPB. Other Cl^- channel blockers, DIDS and IAA-94, also inhibited large LDs formation and Rab8a expression. These results demonstrate that Cl^- channels do not regulate the adipocyte differentiation, but do regulate the LDs formation via Rab8a expression.

.

Keywords

adipose tissue-derived stem cells; adipocyte differentiation; Cl^- channel; lipid droplets; Rab8a

Abbreviations

ASCs, adipose tissue-derived stem cells; LDs, lipid droplets; RUNX2, runt-related transcription factor 2; CFTR, cystic fibrosis transmembrane conductance regulator; TG, triacylglycerol; FA, fatty acid; GLUT4, glucose transporter type 4; ER, endoplasmic reticulum; ADRP, adipose differentiation-related protein; TIP47, tail-interacting protein of 47 kD; HSL, hormone sensitive lipase; PBS, phosphate-buffered saline; DMEM, Dulbecco's modified Eagle Medium; FBS, fetal bovine serum; SMA, smooth muscle actin; FAS, fatty acid synthase; ZONAB, ZO-1 associated nucleic acid binding protein; PPAR-γ, peroxisome proliferator-activated receptor-γ; C/EBPα, CCAAT/enhancer binding protein α; CE, cholesteryl ester; V-ATPase, vacuolar H^+ ATPase.

Introduction

Rabbit adipose tissue-derived stem cells (ASCs) can be differentiated into various cell types, including adipocytes, since they are able to self-renew and have the capacity of multipotent differentiation [1,2]. Additionally, rabbits are widely used as experimental models for human and veterinary medicine by their ease of use and relatively economic maintenance [3]. It has been also reported that lipid metabolism in rabbits is closer to that of humans than that of rodents such as mice and rats [4,5]. Therefore, rabbit ASCs and ASCs-derived adipocyte are considered to be effective cell sources for elucidating of differentiation mechanism and lipid metabolism mechanism.

Cl^- channels have been known to play important roles for the differentiation, cell volume regulation [6], migration [7], proliferation [8], and intracellular acidification [9]. In particular, these channels have been shown to control the differentiation in a variety of cell via the activation of several signaling pathways. For example, ClC-3, which is a voltage-gated Cl^- channel, mediates osteocyte differentiation via the runt-related transcription factor 2 (Runx2) pathway [10]. Runx2 is known as a master transcription factor to regulate osteocyte differentiation [11]. Additionally, it has been also reported that cystic fibrosis transmembrane conductance regulator (CFTR) regulates mesendoderm differentiation from embryonic stem cells via the βcatenin signaling pathway [12]. Furthermore, CLC2 and CLIC4 control the transdifferentiation from fibroblast to myofibroblast via the TGFβ1 signaling pathway [13,14]. However, whether Cl^- channels are involved in adipocyte differentiation from ASCs remains unknown.

Lipid droplets (LDs) are present in most eukaryotic cells, and have been used to evaluate adipocyte differentiation in many studies [15-17]. Triacylglycerol (TG), which is the main component of LDs, is synthesized from fatty acid (FA). FA is synthesized

from glucose taken up by a glucose transporter type 4 (GLUT4), and then becomes TG in the endoplasmic reticulum (ER). The TG surrounded by phospholipid monolayer in the ER is budded as LD from the ER [18]. Phospholipid monolayer-surrounding proteins such as perilipin, adipose differentiation-related protein (ADRP), and tail-interacting protein of 47 kD (TIP47) have important roles in the inhibition of LD lipolysis due to hormone sensitive lipase (HSL) [19]. In particular, the recruitment of perilipin controls the access of lipases to LDs [20]. Furthermore, Rab8a, which is one of the Rab GTPases, has been shown to regulate LDs fusion. Down-regulation of Rab8a decreases the sizes of LDs in 3T3-L1 cells [21]. The sizes of LDs have been linked to the development of obesity, diabetes, and hepatic steatosis [22,23]. However, the molecular mechanism for LDs formation has not been fully elucidated. Furthermore, it has not been determined whether Cl^- channels are associated with LDs formation.

In the present study, I investigated the role of Cl^- channels on adipocyte differentiation and LDs formation, using rabbit ASCs.

Materials and methods

Animals.

This study was carried out under the control of the Animal Care and Use Committee in accordance with the Guidelines for Animal Experiments of Fukushima Medical University (Approval No. 29088). I used 10–12 months old male Japanese white rabbits (3.8–4.0 kg) (Japan Animal Laboratory Inc, Tokyo, Japan) in this study.

Isolation and culture of ASCs.

Adipose tissue isolated from Japanese white rabbits was washed in phosphate-buffered saline (PBS) and treated with 0.1% collagenase type 1A (Sigma-Aldrich, St. Louis, MO, USA) in PBS for 30–40 min at 37℃ with gentle agitation. The cells isolated from adipose tissue were centrifuged at 400×*g* for 5 minutes. The supernatants were discarded and cells were seeded on 35 mm dishes with DMEM, 10% FBS and 1% Penicillin Streptomycin (FUJIFILM Wako Pure Chemical Corporation, Osaka, Japan). When the cells were 80–90% confluent, they were harvested with 0.25% Trypsin-EDTA (FUJIFILM Wako Pure Chemical Corporation), and then used for each experiment.

Adipocyte differentiation of ASCs.

Adipocyte differentiation from ASCs was performed as described previously [24]. Briefly, to differentiate into adipocytes, ASCs were cultured under the condition of adipogenic differentiation medium, which consisted of DMEM, 10% FBS, 10 μM insulin (Sigma-Aldrich), 1 μM dexamethasone (Sigma-Aldrich), 0.5 mM IBMX (Sigma-Aldrich), and 0.1 mM indomethacin (Sigma-Aldrich), for 7 days. Additionally, NPPB (Sigma-Aldrich), DIDS (Sigma-Aldrich), IAA-94 (Sigma-Aldrich) at various

concentrations (1, 10, and 100 μM) and 1 nM Bafilomycin A1 (Cayman Chemical company, Ann Arbor, MI, USA) were added to the culture medium. The culture medium was changed every 2 days. To evaluate the adipogenic differentiation, LDs were stained with BODYPI 493/503 (Thermo Fisher Scientific). Nuclei were stained with HOECHST 33342 (ImmunoChemistry Technologies, Bloomington, MN, USA) and DAPI (Molecular Probes, Eugene, OR, USA). Fluorescent images were observed and acquired using a confocal laser scanning microscopy A1R (Nikon Instech, Chiyoda, Tokyo, Japan).

Measurement of LDs Size.

The diameter of the LDs were measured and analyzed with ImageJ (National Institutes of Health, Bethesda, MD, USA).

Conventional and quantitative real-time RT-PCR.

Total RNA was extracted using an RNeasy Mini kit (Qiagen, Hilden, NW, Germany) according to the manufacturer's protocol. First-strand cDNA was synthesized from 1 μg total RNA using Superscript II reverse transcriptase (TaKaRa Bio, Otsu, Shiga, Japan). Conventional RT-PCR and quantitative real-time RT-PCR was performed as previously described [25]. In quantitative real-time RT-PCR analysis, the expression level of day 0 and control was always defined as 1, and multiple independent data are collected and calculated. The common primer sets are shown in Table 1.

Immunocytochemistry.

ASCs and the differentiated cells were rinsed three times in PBS, and fixed with 4% paraformaldehyde for 30 min. The cells were treated with 0.1% Triton X-100 and 4%

blocking powder in PBS for 30 min at room temperature. After washes with PBS, the cells were stained with specific primary antibodies, Rab8a (1:100, bsm-51077M, Bioss ANTIBODIES, Woburn, MA, USA) and CD44 (1:10, MRB4420, Antigenix america, Huntington Station, NY, USA). The cells were then conjugated with secondary antibodies, Biotinylated Anti-mouse IgG (BA-2000, Vector Laboratories, Burlingame, CA, USA) and Alexa fluor 568 (Molecular Probes), and DAPI. Vectastain ABC-Phycoerithin (Vector Laboratories) was also used. Fluorescent images were observed and acquired using a confocal laser scanning microscopy A1R (Nikon Instech).

Flow cytometry.

The cells were collected into 15 mL tubes and washed with PBS. The cells were centrifuged at 400×*g* for 5 minutes, washed with FACS buffer composed of PBS, 5% BSA and 100 mM EDTA, and incubated with the antibody solution (1:10) for 1 hour at 4℃. The cells were then washed, and the cells were resuspended with FACS buffer. Next, the cells were stained with a secondary antibody conjugated with Alexa fluor 488 (Molecular Probes) at 4℃ for 1 hour. The cells were then centrifuged and washed three times in the FACS buffer. A total of 1×10^6 cells/ml were analyzed using a FACSCanto Ⅱ flow cytometer (Becton, Dickinson and Company, Franklin Lakes, NJ, USA).

Measurement of intracellular pH.

The intracellular pH of the differentiated cells from ASCs was measured using BCECF-AM (DOJINDO LABORATORIES, Kamimashiki, Kumamoto, Japan), according to the manufacturer's instructions and previousreport [26].

Statistical analysis.

All experiments were performed independently at least three times. Data are expressed as means ± SD. All statistical significance was verified using the Mann-Whitney *U*-test or Bonferroni. *P* values < 0.05 were considered statistically significant.

Results

Characterization of ASCs isolated from adipose tissue

The cells isolated from adipose tissue showed the typical morphology of ASCs (Figure 1A). To confirm the characteristics of the ASCs, RT-PCR using various markers was carried out. The expression of ASC markers *CD44*, S*mooth muscle actin* (*SMA*), and *Vimentin* was detected (Figure 1B). Furthermore, it was confirmed that the CD44 was localized at the cell membrane by immunostaining (Figure 1C). Flow cytometry analysis showed that CD44-positive cells were 89.5% in all cells (Figure 1D). These findings showed that the cells isolated from adipose tissue had the phenotype of the ASCs.

Generation of adipocytes from ASCs

The ASCs were cultured with an adipogenic differentiation medium for 7 days in order to differentiate into adipocytes (Figure 2A). The morphology of the differentiated cells from the ASCs was spherical (Figure 2B (a) and (b)). In addition, to visualize the LDs, the cells were stained with BODIPY 493/503. The sizes of the LDs in the differentiated cells increased by approximately two times compared to those of the ASCs (Figure 2C (a), (b), and D). To investigate whether the expression of the adipocyte markers could be detected in the differentiated cells from the ASCs, real-time RT-PCR using several markers was performed. The expression levels of ASCs markers *CD44, SMA,* and *Vimentin* were decreased during the differentiation process (Figure 2E (a)-(c)). On the other hand, adipocyte markers *Fatty acid synthase* (*FAS*)*, perilipin,* and *adiponectin* were significantly up-regulated (Figure 2E (d)-(f)). These results showed that ASCs could be differentiated into adipocytes with an adipogenic differentiation medium.

The role of Cl^- channels during adipocyte differentiation from ASCs

I induced the ASCs into adipocytes using NPPB, a Cl^- channel blocker, to investigate the role of the Cl^- channels on adipocyte differentiation. The morphology of the differentiated cells treated with NPPB was similar to that of those untreated with NPPB (Figure 3A (a) and (b)). Next, to compare the expression levels of adipocyte markers in the differentiated cells treated with NPPB to those untreated with NPPB, real-time RT-PCR was performed. The expression levels of ASCs markers *CD44, SMA,* and *Vimentin* had no significant differences between the differentiated cells treated with NPPB and those untreated with NPPB (Figure 3B (a)-(c)). Furthermore, the expression levels of adipocyte markers *FAS* and *adiponectin* had also no significant differences between the groups (Figure 3B (d) and (f)). Interestingly, the expression levels of LD-binding protein *perilipin* in the differentiated cells treated with NPPB were higher than those untreated with NPPB (Figure 3B (e)). Next, LDs were visualized in the differentiated cells with fluorescent dyes. Large LDs were found in the differentiated cells untreated with NPPB (Figure 3C (a)). On the other hand, NPPB decreased LDs sizes in a concentration-dependent manner (Figure 3C (b) and D). However, NPPB is known not only as a Cl^- channel blocker, but also as an agonist of GPR35 [27]. Thus, LD formation and sizes were investigated using several Cl^- channel blockers. Other Cl^- channel blockers, DIDS and IAA-94, also inhibited large LDs formation and decreased the LDs sizes (Figure 3C (c), (d), and D). In particular, large LD formation tended to be inhibited, when the differentiated cells were treated with 100 μM NPPB or IAA-94. Thus, these results indicated that Cl^- channel blocker did not inhibit adipocyte differentiation, but inhibited large LDs formations.

The role of Cl^- channels on LDs formations via Rab8a expression

To investigate the molecular mechanisms of impaired LDs formation in the differentiated cells treated with Cl^- channel blocker, I confirmed the expression of Rab8a, which is known as a regulator of LDs fusion [21], using real-time RT-PCR. Interestingly, *Rab8a* expression was significantly down-regulated in the differentiated cells treated with Cl^- channel blocker (Figure 4A). To precisely examine whether Rab8a expression was decreased in the differentiated cells treated with Cl^- channel blocker, the cells were evaluated using immunofluorescent staining with Rab8a antibody. The localization of Rab8a was partially consistent with LDs in the differentiated cells untreated with Cl^- channel blocker (Figure 4B (a)). On the other hand, Rab8a expression was decreased in the differentiated cells treated with Cl^- channel blocker (Figure 4B (b)-(d)). Interestingly, Rab8a expression levels and LDs sizes were significantly decreased in the differentiated cells treated with Bafilomycin, which is a vacuolar H^+ ATPase (V-ATPase) inhibitor (Figure 4C-E). Furthermore, the intracellular pH value of the differentiated cells treated with Bafilomycin was shifted to acidic side due to the inhibition of V-ATPase function. Additionally, that of the differentiated cells treated with Cl^- channel blocker was also shifted to acidic side (Figure 4F). These results suggest that Cl^- channels regulate the lysosomal acidification and the LDs formation via Rab8a expression (Figure 5).

Discussion

In the present study, I revealed that Cl^- channels do not regulate the adipocyte differentiation, but do regulate LDs formation via Rab8a expression. While several research groups have reported that the Cl^- channels control the differentiation of some cell types, there have been no reports about the roles of Cl^- channels on adipocyte differentiation from ASCs. To my knowledge, this is the first report focusing on the role of Cl^- channels during adipocyte differentiation.

Cl^- channels have been known to play an important role in the differentiation of some cell types. ClC-3 mediates osteocyte differentiation via the Runx2 pathway [10]. CFTR controls epithelial differentiation through modulation of the ZO-1 associated nucleic acid binding protein (ZONAB) pathway [28]. Therefore, morphological change such as differentiation is strongly impacted by intracellular signaling activation through Cl^- channels. In the current study, I examined the role of Cl^- channels on adipocyte differentiation, using ASCs.

First, I induced ASCs into adipocytes according to a previously described protocol [24]. FAS plays a central role in LDs formation in mammalian species through the conversion of acetyl-CoA and malonyl-CoA to palmitate. Additionally, perilipin, which is a LD-binding protein, can inhibit LD lipolysis due to HSL [19]. Adiponectin protein synthesis and secretion occurred specifically in mature adipocytes and thus serve as a distinctive marker of adipocyte differentiation [29]. Thus, I examined the expression of *FAS*, *perilipin*, and *adiponectin* by real-time RT-PCR analysis. These genes were up-regulated during differentiation process (Figure 2E (d)-(f)). Furthermore, I indicated that the number and sizes of the LDs were increased in the differentiated cells (Figure 2C and D). Next, since it has been reported that the stem cell differentiation is strongly impacted

by Cl^- channels [12], I induced ASCs into adipocytes using Cl^- channel blocker to confirm whether Cl^- channels are involved in adipocyte differentiation. Real-time RT-PCR analysis showed that the expression levels of *FAS* and *adiponectin* had no significant differences between the differentiated cells treated with and without Cl^- channel blocker (Figure 3B (d) and (f)). However, the expression levels of *perilipin* in the differentiated cells treated with Cl^- channel blocker were higher than that in those untreated with Cl^- channel blocker (Figure 3B (e)). Since the number of small LDs was increased in the differentiated cells treated with Cl^- channel blocker, there is a possibility that the expression levels of *perilipin* were also increased. Surprisingly, LDs sizes were significantly decreased in the differentiated cells treated with Cl^- channel blocker (Figure 3C and D). Thus, these results indicate that Cl^- channels do not regulate the adipocyte differentiation, but do regulate the LDs formation.

The Rab family of small GTPases has been known to regulate multiple steps of membrane trafficking. Previous studies have suggested that Rab species on LDs could regulate interaction of LDs with a specific organelle [18,30]. In particular, Rab8a has been shown to regulate LDs fusion. Down-regulation of Rab8a decreases the sizes of LDs in 3T3-L1 cells [21]. Therefore, I examined the expression levels of Rab8a using real-time RT-PCR. The expression levels of *Rab8a* were significantly down-regulated in differentiated cells treated with Cl^- channel blocker (Figure 4A). Immunocytochemistry also showed that the expression of Rab8a was decreased in differentiated cells treated with Cl^- channel blocker (Figure 4B (b)-(d)). These results indicate that Cl^- channels regulate the LDs formation via Rab8a expression.

Lysosomes contain various hydrolytic enzymes and maintain luminal acidic pH values for efficient function. TG and cholesteryl ester (CE) taken up by endocytosis are

hydrolyzed under the appropriate acidic environment in the lysosomes, and are then used as sources for LDs formation. Although reasonable acidification is mediated by a vacuolar H^+ ATPase (V-ATPase), a parallel anion pathway via the CLC Cl^- channel is essential to allow bulk proton transport [31,32]. In the current study, it is thought that the function of the CLC Cl^- channel, which is the target of Cl^- channel blocker, is suppressed, and proton transport by V-ATPase may be also suppressed. Thus, I examined the role of lysosomal acidification on LDs formation, using Bafilomycin. Interestingly, Rab8a expression levels and LDs sizes were significantly decreased in the differentiated cells treated with Bafilomycin (Figure 4C-E). Additionally, the intracellular pH value of the differentiated cells treated with Bafilomycin or Cl^- channel blocker was shifted to acidic side (Figure 4F). Therefore, it is considered that the lysosomal acidification was also involved in LDs formation (Figure 5).

In conclusion, this study suggests that the Cl^- channels are not involved in adipocyte differentiation. On the other hand, these channels regulate the LDs formation via Rab8a expression. To my knowledge, it is the first report to clarify the role of Cl^- channels during adipocyte differentiation. Since the number and sizes of the LDs in adipocytes cause obesity, which is a major risk factor for noninsulin-dependent diabetes mellitus, cardiovascular diseases, and hypertension [22,23], further investigation is required to elucidate the molecular mechanisms of LDs formation.

Disclosure statement

The authors declare no conflicts of interest.

Funding

This study was supported by Fukushima Medical University.

References

[1] Li H, Xu Y, Fu Q, et al. Effects of multiple agents on epithelial differentiation of rabbit adipose-derived stem cells in 3D culture. Tissue Eng Part A. 2012;18:1760-1770.

[2] Barretto LS, Lessio C, Nakamura AN, et al. Cell kinetics, DNA integrity, differentiation, and lipid fingerprinting analysis of rabbit adipose-derived stem cells. In Vitro Cell Dev Biol Anim. 2014;50:831-839.

[3] Intawicha P, Ou YW, Lo NW, et al. Characterization of embryonic stem cell lines derived from New Zealand white rabbit embryos. Cloning Stem Cells. 2009;11:27-38.

[4] Fan J, Kitajima S, Watanabe T, et al. Rabbit models for the study of human atherosclerosis:
from pathophysiological mechanismsto translational medicine. Pharmacol Ther. 2015;146:104-119.

[5] Zhang XJ, Chinkes DL, Aarsland A, et al. Lipid metabolism in diet-induced obese rabbits is similar to that of obese humans. J Nutr. 2008;138:515-518.

[6] Hazama A, Okada Y. Ca^{2+} sensitivity of volume-regulatory K^+ and Cl^- channels in cultured human epithelial cells. J Physiol. 1988;402:687-702.

[7] Schwab A, Fabian A, Hanley PJ, et al. Role of ion channels and transporters in cell migration. Physiol Rev. 2012;92:1865-1913.

[8] Guan YY, Wang GL, Zhou JG. The ClC-3 Cl^- channel in cell volume regulation, proliferation and apoptosis in vascular smooth muscle cells. Trends Pharmacol Sci. 2006;27:290-296.

[9] Edwards JC, Kahl CR. Chloride channels of intracellular membranes. FEBS Lett. 2010;584:2102-2111.

[10] Wang H, Mao Y, Zhang B, et al. Chloride channel ClC-3 promotion of

osteogenic differentiation through Runx2. J Cell Biochem. 2010;111:49-58.

[11] Chen Q, Shou P, Zheng C, et al. Fate decision of mesenchymal stem cells: adipocytes or osteoblasts?. Cell Death Differ. 2016;23:1128-1139.

[12] Liu Z, Guo J, Wang Y, et al. CFTR-β-catenin interaction regulates mouse embryonic stem cell differentiation and embryonic development. Cell Death Differ. 2017;24:98-110.

[13] Sun L, Dong Y, Zhao J, et al. The ClC-2 chloride channel modulates ECM synthesis, differentiation, and migration of human conjunctival fibroblasts via the PI3K/AKT signaling pathway. Int J Mol Sci. 2016;17:E910.

[14] Shukla A, Edwards R, Yang Y, et al. CLIC4 regulates TGF-β-dependent myofibroblast differentiation to produce a cancer stroma. Oncogene. 2014;33:842-850.

[15] Zomer HD, Roballo KC, Lessa TB, et al. Distinct features of rabbit and human adipose-derived mesenchymal stem cells: implications for biotechnology and translational research. Stem Cells Cloning. 2018;11:43-54.

[16] Takahashi Y, Shinoda A, Furuya N, et al. Perilipin-mediated lipid droplet formation in adipocytes promotes sterol regulatory element binding protein-1 processing and triacylglyceride accumulation. PLoS One. 2013;8:e64605.

[17] Gerlach JC, Lin YC, Brayfield CA, et al. Adipogenesis of human adipose-derived stem cells within three-dimensional hollow fiber-based bioreactors. Tissue Eng Part C Methods. 2012;18:54-61.

[18] Guo Y, Cordes KR, Farese RV, et al. Lipid droplets at a glance. J Cell Sci. 2009;122:749-752.

[19] Fujimoto T, Ohsaki Y, Cheng J, et al. Lipid droplets: a classic organelle with new outfits. Histochem Cell Biol. 2008;130:263-279.

[20] Tansey JT, Sztalryd C, Hlavin EM, et al. The central role of perilipin A in lipid metabolism and adipocyte lipolysis. IUBMB Life. 2004;56:379-385.

[21] Wu L, Xu D, Zhou L, et al. Rab8a-AS160-MSS4 regulatory circuit controls lipid droplet fusion and growth. Dev Cell. 2014;30:378-393.

[22] Parlee SD, Lentz SI, Mori H, et al. Quantifying size and number of adipocytes in adipose tissue. Methods Enzymol. 2014;537:93-122.

[23] Hajer GR, Van Haeften TW, Visseren FL. Adipose tissue dysfunction in obesity, diabetes, and vascular diseases. Eur Heart J. 2008;29:2959-2971.

[24] Zuk PA, Zhu M, Ashjian P, et al. Human adipose tissue is a source of multipotent stem cells. Mol Biol Cell. 2002;13:4279-4295.

[25] Yoshie S, Imaizumi M, Nakamura R, et al. Generation of airway epithelial cells with native characteristics from mouse induced pluripotent stem cells. Cell Tissue Res. 2016;364:319-330.

[26] Kobayashi D, Kakinouchi K, Nagae T, et al. Cesium reversibly suppresses HeLa cell proliferation by inhibiting cellular metabolism. FEBS Lett. 2017;591:718-727.

[27] Taniguchi Y, Tonai-Kachi H, Shinjo K. 5-Nitro-2-(3-phenylpropylamino)benzoic acid is a GPR35 agonist. Pharmacology. 2008;82:245-249.

[28] Ruan YC, Wang Y, Silva N, et al. CFTR interacts with ZO-1 to regulate tight junction assembly and epithelial differentiation through the ZONAB pathway. J Cell Sci. 2014;127:4396-4408.

[29] Körner A, Wabitsch M, Seidel B, et al. Adiponectin expression in humans is dependent on differentiation of adipocytes and d own-regulated by humoral serum components of high molecular weight. Biochem Biophys Res Commun. 2005;337:540-50.

[30] Liu P, Bartz R, Zehmer JK, et al. Rab-regulated membrane traffic between adiposomes and multiple endomembrane systems. Methods Enzymol. 2008;439:327-337.

[31] Ohkuma S, Moriyama Y, Takano T. Identification and characterization of a proton pump on lysosomes by fluorescein-isothiocyanate-dextran fluorescence. Proc Natl Acad Sci USA. 1982;79:2758-2762.

[32] Graves AR, Curran PK, Smith CL, et al. The Cl-/H+ antiporter ClC-7 is the primary chloride permeation pathway in lysosomes. Nature. 2008;453:788-792.

Table 1. Primer sets used for conventional RT-PCR and quantitative real-time RT-PCR

Gene	Sense primer	Antisense primer	Annealing	Product size
CD44	tcgcggtcaacagtcgaaga	cctgagacttgctggcttct	60	119
SMA	tgctgaccgtatgcagaagg	cggcttcatcgtactcctgt	60	169
Vimentin	actaatctggaatcactccc	aaggtcatcgtgatgctgag	60	119
FAS	actacatagccaagtgtctg	ctgagtaactgagaagcgta	60	179
Perilipin	cacatcgagtcacgtactct	cttaaaggagccagcattgc	60	162
Adiponectin	gcaggttggatagcaggcat	gaccttcagctccagtcact	60	182
Rab8a	cgtgaacgacaagcgacaag	tgaagaaggcgttctccacg	60	109
GAPDH	cgtctcctgcgacttcaaca	ataccaggaaatgagcttca	60	119

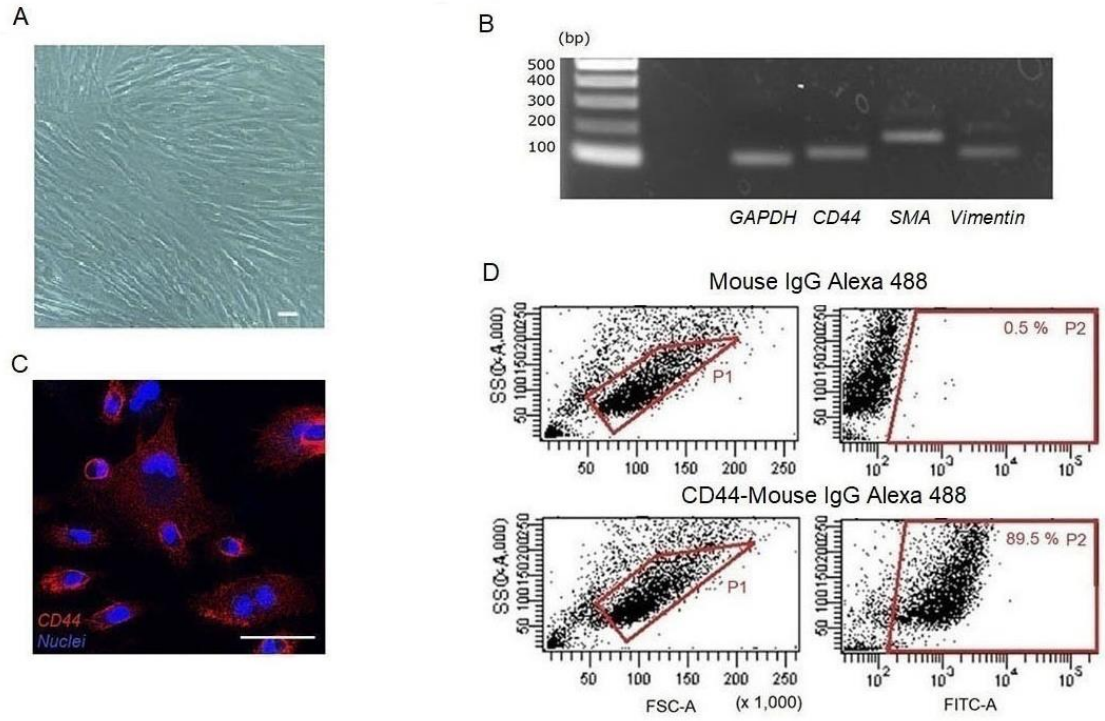

Figure 1. Characterization of ASCs isolated from adipose tissue. A: Representative phase contrast images at passage 3. Bars indicate 50 μm. B: Genetic characterization of ASCs. RT-PCR analysis of gene expression in undifferentiated markers. C: Immunostaining of ASCs with the use of anti-CD44 antidody. Nuclei were stained with DAPI. Bars indicate 50 μm. D: Flow cytometric analysis of ASCs using CD44 antibody.

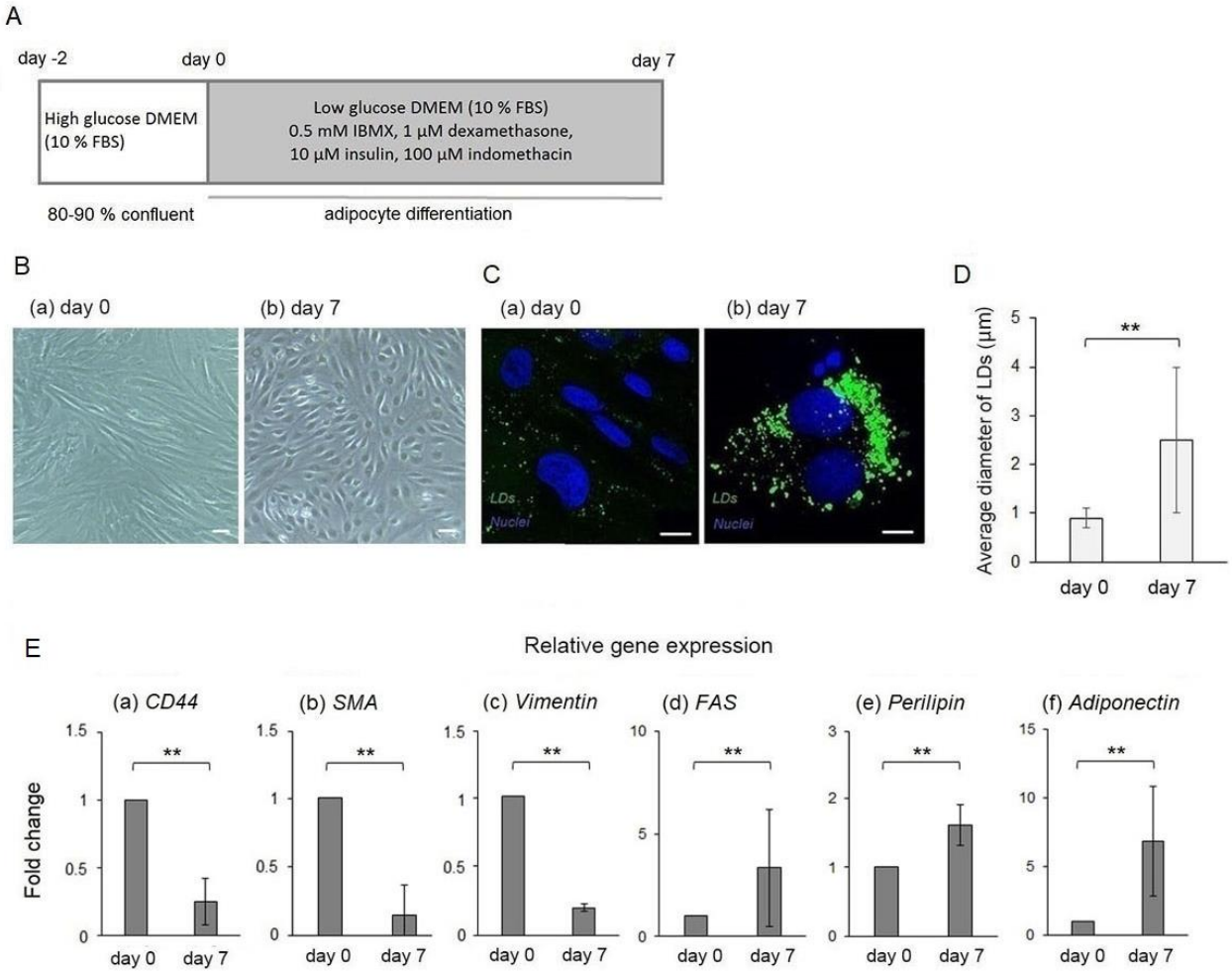

Figure 2. Generation of adipocytes from ASCs. A: Time course for the generation of adipocytes from ASCs. B: Phase contrast images at day 0 (a) and day 7 (b). Bars indicate 50 µm. C: Fluorescent staining of undifferentiated ASCs on day 0 (a) and differentiated cells on day 7 (b) using BODIPY 493/503. Bars indicate 10 µm. D: Quantitative data of LDs size. Data are expressed as means ± SD. Statistical significance was verified using the Mann-Whitney *U*-test (n=25, ***P*<0.01 vs. undifferentiated ASCs on day 0). E: Quantitative gene expression of various markers (undifferentiated markers, a-c; adipocyte markers, d-f) during the course of differentiation. Samples were obtained from

undifferentiated ASCs on day 0 and differentiated cells on day 7. Relative expression levels of each gene to *GAPDH* were compared with those of undifferentiated ASCs on day 0. Data are expressed as means ± SD. Statistical significance was verified using the Mann-Whitney *U*-test (n≧3, ***P*<0.01 vs. undifferentiated ASCs on day 0).

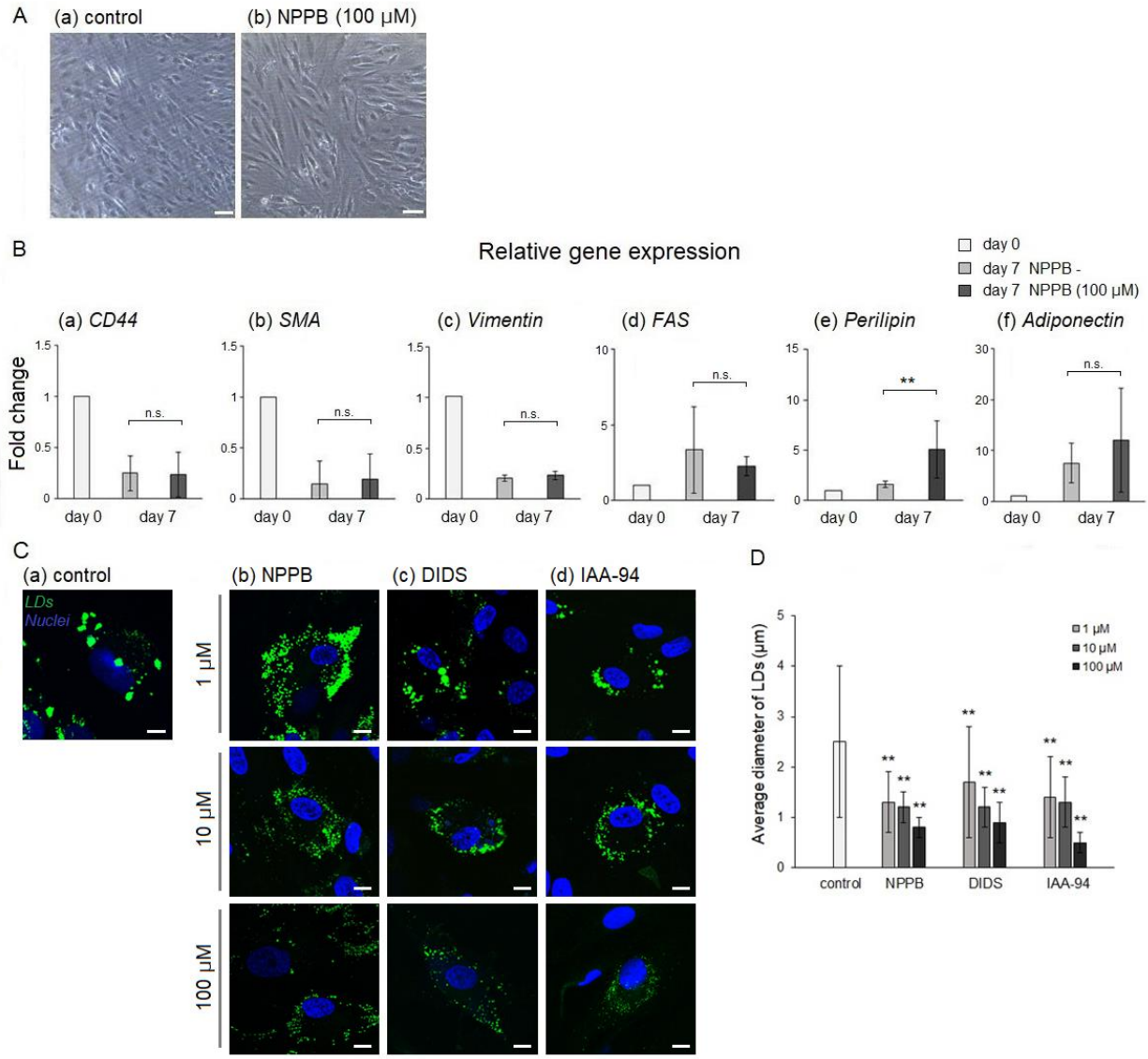

Figure 3. Effects of Cl^- channel blocker during the adipocyte differentiation. A: Phase contrast images of differentiated cells untreated with NPPB (a) and treated with NPPB (b). Bars indicate 50 μm. B: Quantitative gene expression of various markers (undifferentiated markers, a–c; adipocyte markers, d–f) during the differentiation. Samples were obtained from undifferentiated ASCs on day 0 and differentiated cells untreated with NPPB and treated with NPPB on day 7. Relative expression levels of each gene to *GAPDH* were compared with those of undifferentiated ASCs on day 0. Data are

expressed as means ± SD. Statistical significance was verified using the Bonferroni (n≧3, **P<0.01). C: Fluorescent staining of differentiated cells untreated with Cl^- channel blocker (a) and treated with Cl^- channel blocker at various concentrations (b-d) on day 7 using BODIPY 493/503. Bars indicate 10 μm. D: Quantitative data of LDs size. Data are expressed as means ± SD. Statistical significance was verified using the Bonferroni (n=25, **P< 0.01 vs. differentiated cells untreated with Cl^- channel blocker).

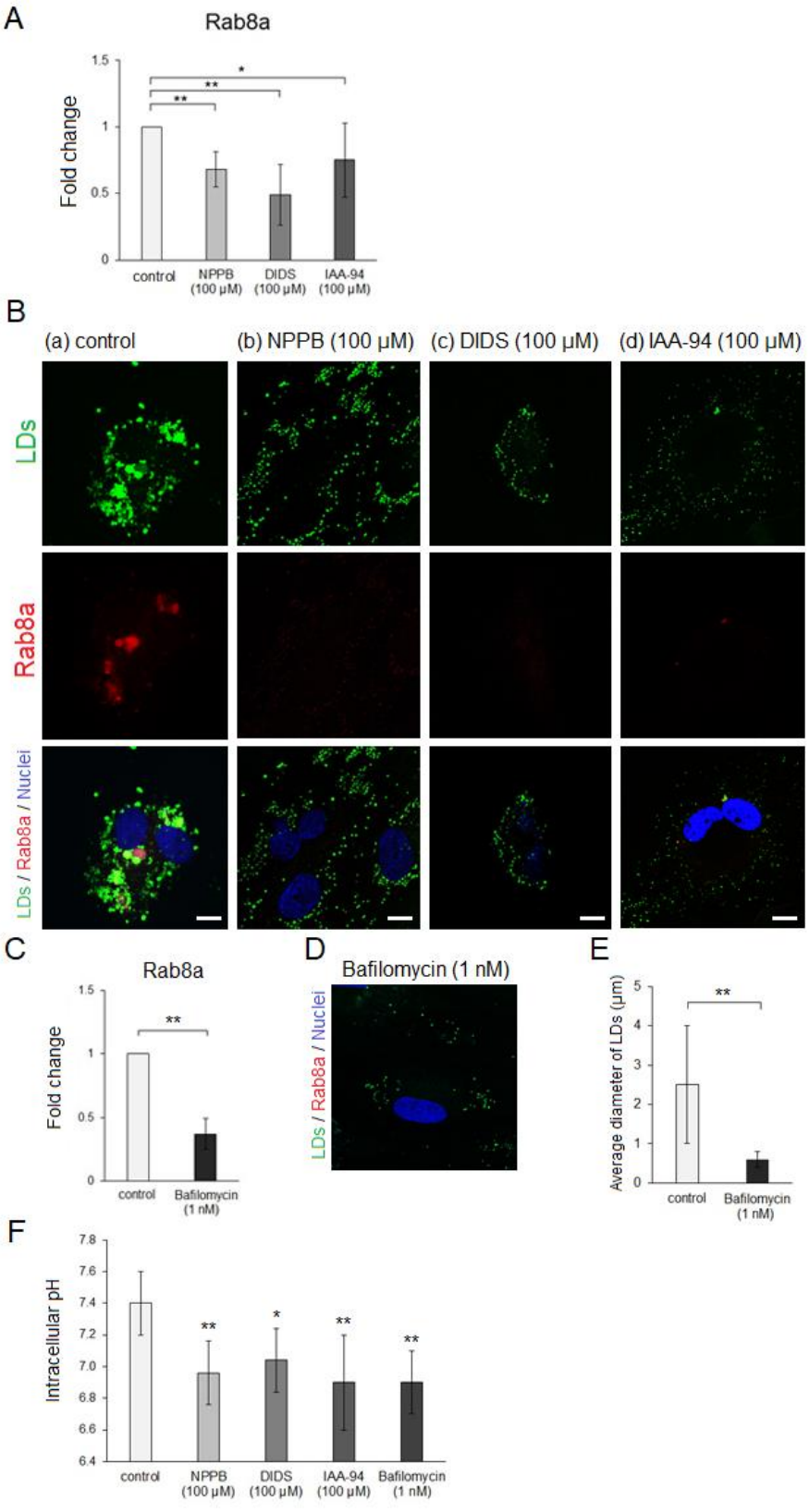
A
Rab8a
Fold change
1.5
1
0.5
0
*
**
**
control
NPPB (100 μM)
DIDS (100 μM)
IAA-94 (100 μM)
B
(a) control
(b) NPPB (100 μM)
(c) DIDS (100 μM)
(d) IAA-94 (100 μM)
LDs
Rab8a
LDs / Rab8a / Nuclei
C
Rab8a
Fold change
1.5
1
0.5
0
**
control
Bafilomycin (1 nM)
D
Bafilomycin (1 nM)
LDs / Rab8a / Nuclei
E
Average diameter of LDs (μm)
5
4
3
2
1
0
**
control
Bafilomycin (1 nM)
F
Intracellular pH
7.8
7.6
7.4
7.2
7.0
6.8
6.6
6.4
**
*
**
**
control
NPPB (100 μM)
DIDS (100 μM)
IAA-94 (100 μM)
Bafilomycin (1 nM)

Figure 4. LDs formation via Rab8a. A: Quantitative gene expression of Rab8a. Data are expressed as means ± SD. Statistical significance was verified using the Bonferroni (n≧4, $^{**}P< 0.01$ and $^{*}P< 0.05$ vs. differentiated cells untreated with Cl^- channel blocker). Samples were obtained from differentiated cells untreated with Cl^- channel blocker and treated with Cl^- channel blocker on day 7. B: Immunostaining of the differentiated cells with the use of Rab8a antibody. Nuclei were stained with DAPI, and LDs were stained with BODIPY 493/503. Bars indicate 10 μm. C: Quantitative gene expression of Rab8a. Data are expressed as means ± SD. Statistical significance was verified using the Mann-Whitney *U*-test (n≧4, $^{**}P<0.01$ vs. differentiated cells untreated with Bafilomycin). D: Immunostaining of the differentiated cells with the use of Rab8a antibody. Nuclei were stained with DAPI, and LDs were stained with BODIPY 493/503. Bars indicate 10 μm. E: Quantitative data of LDs size. Data are expressed as means ± SD. Statistical significance was verified using the Mann-Whitney *U*-test (n=25, $^{**}P<0.01$ vs. differentiated cells untreated with Bafilomycin). F: The intracellular pH of the differentiated cells treated with Cl^- channel blocker and Bafilomycin using a calibration curve ranging from pH 6.0–8.0. Data are expressed as means ± SD. Statistical significance was verified using the Bonferroni (n≧5, $^{**}P<0.01$ and $^{*}P< 0.05$ vs. differentiated cells untreated with Cl^- channel blocker).

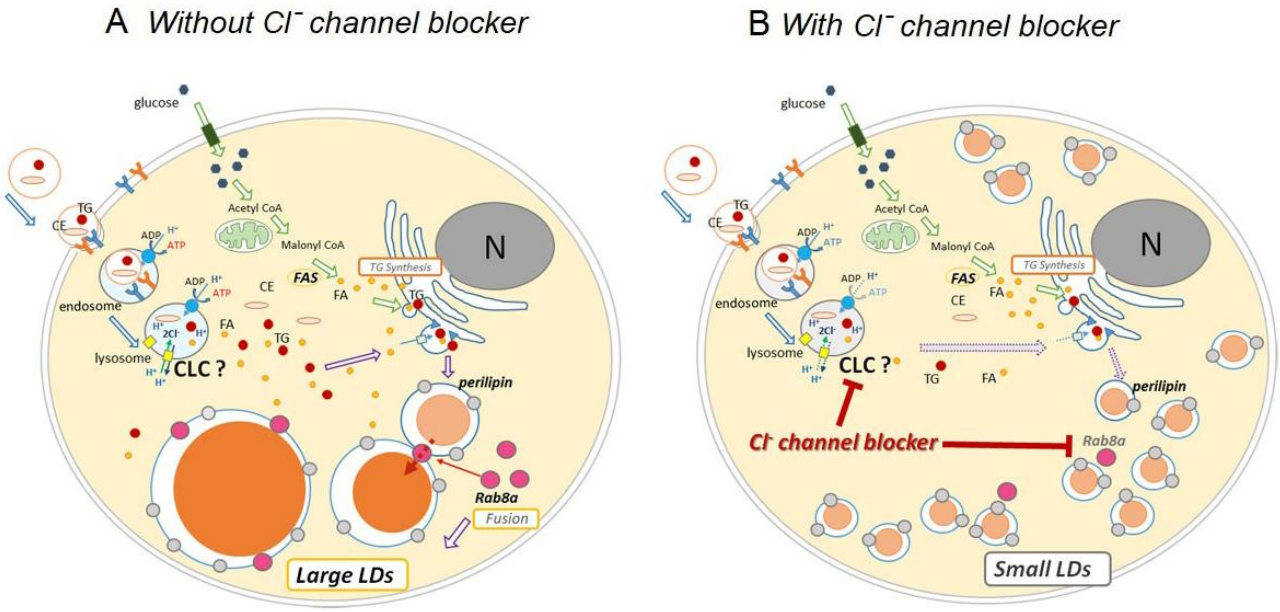

Figure 5. Schema of molecular mechanisms for LDs formation. A: LDs formation of the differentiated cells untreated with Cl^- channel blocker. B: LDs formation of the differentiated cells treated with Cl^- channel blocker. Formation of large LDs via Rab8a is inhibited by Cl^- channel blocker.

Acknowledgements

I thank Prof. Ikuo Wada (Department of Cell Science, School of Medicine, Fukushima Medical University, Fukushima, Japan), Prof. Akihiro Hazama, Dr. Shinichiro Katsuda, Dr. Susumu Yoshie, Dr. Masao Miyake, and Ms. Natsumi Nishimura (Department of Cellular and Integrative Physiology, School of Medicine, Fukushima Medical University, Fukushima, Japan) for their technical support, and for allowing me use their equipment.